

# Semiconductor detectors in simulations and experiments

Christian Bourjau

January 11, 2016

Semiconductor based detectors are indispensable components in most modern particle detectors. In particular Silicon (Si) is the material of choice for the detectors closest to the interaction point in all four major LHC experiments. The reason for this choice is manifold. Semiconductor detectors can be build very compact, due to their large material density. But they also offer a high energy and spatial resolution, reasonably good radiation hardness and fast timing characteristics [3].

## 1 Theory

Semiconductor detectors exploit the properties of pn junctions. In the simplest consideration, a pn-junction can be regarded as a one dimensional contact between a p and an n doped semiconductor. Once the contact is made, charge carriers diffuse from the n doped component to the p doped one and vice versa creating a build in potential. The result of this process is the creation of a so called depletion zone around the contact within which no free charge carriers are present. Equilibrium is reach once the build in potential counterbalances the diffusion of charges. Assuming that the donor and acceptor concentrations behave like  $N_A \gg N_D$ , the build in potential is given by [1]

$$\Psi_0 = \frac{k_B T}{q} \ln \left( \frac{N_A N_D}{n_i^2} \right) \quad (1)$$

where  $k_B$  is the Boltzmann constant,  $T$  the temperature and  $q$  is the elementary charge.

Using the same assumption of asymmetric doping, the width  $d$  of the depletion area is given by [3]

**Table 1:** Simulation based results for the various parameters of the pn junction under variation of temperature.  $N_A = 1 \times 10^{15}$  and  $N_D = 1 \times 10^{10}$  theoretical predictions are given where applicable

Temperature [K]	200	300	400
Build in potential $\Psi_0$ [V]	0.629	0.312	0.176
Maximal E-field $E_{\max}$ [ $\text{Vm}^{-1}$ ]	6.612	8.902	11.139
Width depletion region [ $\mu\text{m}$ ]	1.903	0.701	0.316
Build in potential (theo.) [V]	-	0.278	-
Width depletion region (theo.) [ $\mu\text{m}$ ]	-	0.607	-

unfeasible since  $n(i)$  for silicon is  $1.5 * 10^{10}$  at 300K

$$d \approx \sqrt{\frac{2\epsilon_0\epsilon_S(\Psi_0 + V_R)}{qN_A}} \quad (2)$$

where  $\epsilon_0$  and  $\epsilon_S$  are the permittivity constants of the vacuum and of the semiconductor respectively and  $V_R$  is an optionally applied voltage. However, since the  $d$  proved to be a parameter which is not easily accessible in the gss output it is helpful to derive it based on the maximal field  $E_{\max}$  strength within the junction [3]:

$$d = \frac{2(\Psi_0 + V_R)}{E_{\max}} \quad (3)$$

OK

## 2 Simulations

The following simulations were conducted using the freely available gss [2] software.

### 2.1 PN junction

In the first exercise, a pn junction between two  $50 \mu\text{m}$  wide and deep regions was modeled.

The following summarizes the effect of a variation in temperature, donor/acceptor concentration and material.

The results in Tab. 1 exhibit the effect of a change in temperature. Namely, three simulations were conducted at 200, 300 and 400 K. Theoretical predictions are only available for the 300 K case. Notably, the depleted region and build-in potential was found to decrease with an increase in temperature, while  $E_{\max}$  increase in that case.

**Table 2:** Simulation based results for the various parameters of the pn junction under variation of acceptor concentration.  $T = 300$  K and  $N_D = 1 \times 10^{10}$  theoretical predictions are given where applicable

Acceptor concentration $N_A$	$1 \times 10^{14}$	$1 \times 10^{15}$	$1 \times 10^{16}$
Build in potential $\Psi_0$ [V]	0.253	0.312	0.372
Maximal E-field $E_{\max}$ [ $\text{Vm}^{-1}$ ]	4.085	8.902	23.097
Width depletion region [ $\mu\text{m}$ ]	1.239	0.701	0.322
Build in potential (theo.) [V]	0.218	0.278	0.338
Width depletion region (theo.) [ $\mu\text{m}$ ]	1.702	0.607	0.212

should probably be [Vum-1], otherwise result wrong by O E6

**Table 3:** Simulation based results of a pn junction based on Si or Ge.  $T = 300$  K,  $N_A = 1 \times 10^{15}$ ,  $N_D = 1 \times 10^{10}$  where used in both cases. Theoretical predictions are given for comparison.

Material	Si	Ge
Build in potential $\Psi_0$ [V]	0.312	0.0980
Maximal E-field $E_{\max}$ [ $\text{Vm}^{-1}$ ]	8.902	6.9519
Width depletion region [ $\mu\text{m}$ ]	0.701	0.282
Build in potential (theo.) [V]	0.278	0.074
Width depletion region (theo.) [ $\mu\text{m}$ ]	0.607	0.099

Tab. 2 summarized the results for a variation in acceptor concentration. It was found that an increase in  $N_A$  leads to a decrease in  $\Psi_0$  and  $d$  in both simulation and theoretical values.

Lastly, the influence of the used bulk material was investigated and the results are displayed in Tab. 3. Note that the intrinsic charge carrier density is significantly different for the two materials ( $n_i^{Si} = 1.5 \times 10^{10} \text{ cm}^{-3}$  and  $n_i^{Ge} = 2.4 \times 10^{13} \text{ cm}^{-3}$ ). Interestingly, this increase in charge carrier density lead to a decrease of the depletion width and build in potential, but the simulations yielded also a decreased  $E_{\max}$  for Ge. Note, that an increase in temperature as well as an increase in  $N_A$  increase the number of available charge carries. Therefore, it was surprising to see that the effect caused by the change to a material with a larger charge carrier density did not yield analogous results with respect to  $E_{\max}$  as an increase in  $T$  or  $N_A$ .

## IV-curve

In the following, an IV scan was conducted on a pn diode. The diodes had had the dimensions  $50\ \mu\text{m} \times 100\ \mu\text{m}$ , whereby the contacts were at the far sides. The cathode was connected to an n-doped bulk region of  $97\ \mu\text{m}$  thickness and doping concentration of  $1 \times 10^{12}\ \text{cm}^{-3}$ . The anode was attached to the  $3\ \mu\text{m}$  acceptor part of the diode which was doped at  $5 \times 10^{18}\ \text{cm}^{-3}$ . Fig. 1 (Fig. 2) display the IV curves for the reverse (forward) bias for Si (Ge). Rearranging eq. (2) for the depletion voltage yields theoretical predictions for the  $V_R^{Si} = 34.851\ \text{V}$  and  $V_R^{Ge} = 35.115\ \text{V}$  at 300 K. The simulated depletion voltages were found to be  $\sim 10\ \text{V}$  for the afore mentioned parameters. It is not clear where this discrepancy stems from.

Concerning the forward bias, both bulk materials clearly exhibit the transition to forward conduction at  $\sim -1\ \text{V}$ . After this point the simulation shows the expected linear dependence of the current to the applied voltage.

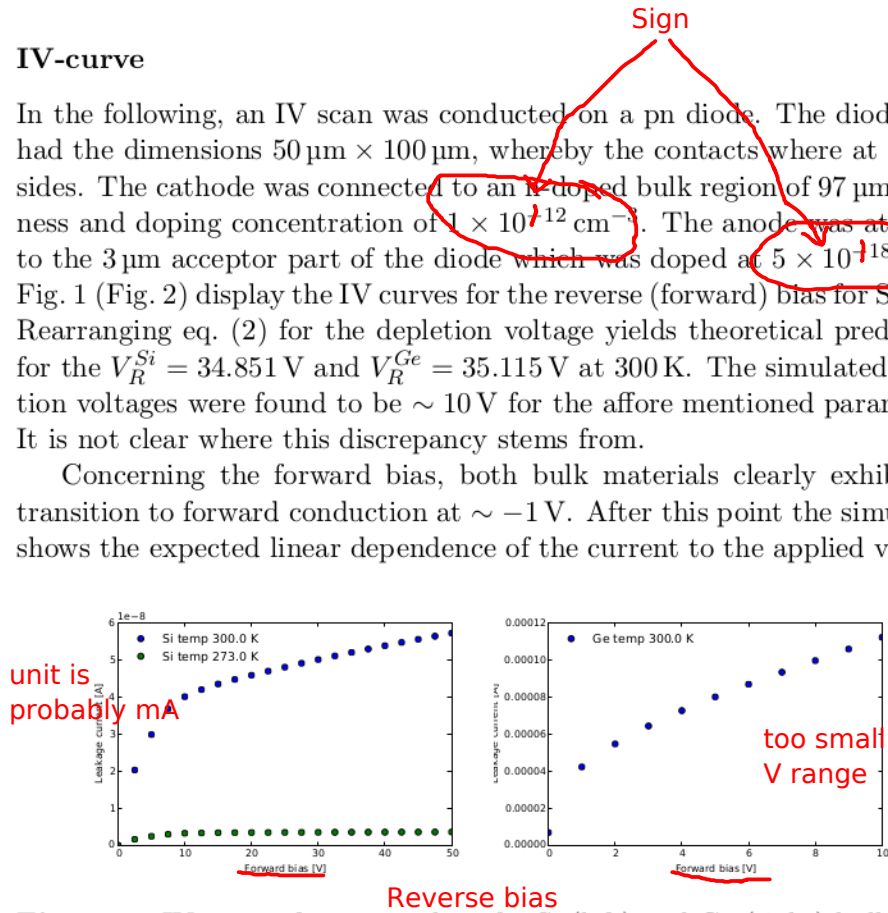


**Figure 1:** IV curves for reverse bias for Si (left) and Ge (right) bulk material.

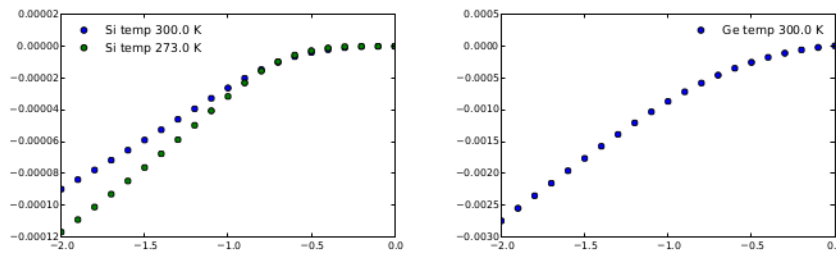


**Figure 2:** IV curves for forward bias for Si (left) and Ge (right) bulk material.

## 2.2 Schottky diode

The gss simulation software was also used to study the properties of a Schottky diode. The dimensions of the Schottky diode were adopted to be comparable to those used for the pn diode. Namely, the  $1 \times 10^{12} \text{ cm}^{-3}$  p-doped bulk region was set to extend over  $100 \mu\text{m}$ . One end of this bulk region was used as the cathode, while the opposite end one was simulated as a Schottky anode. Despite the differences in geometry, it was found that the Schottky diode had a qualitatively similar response to changes in temperature as the previously simulated pn diode. Namely, an increase of the E-field and a decrease of the depletion width were observed for a rise in temperature. The IV curves for forward (left) and reverse (right) bias are shown in Fig. 3. The forward bias shows the expected linear behavior while the reverse one exhibits a full depletion current at  $\sim -50 \text{ V}$ .

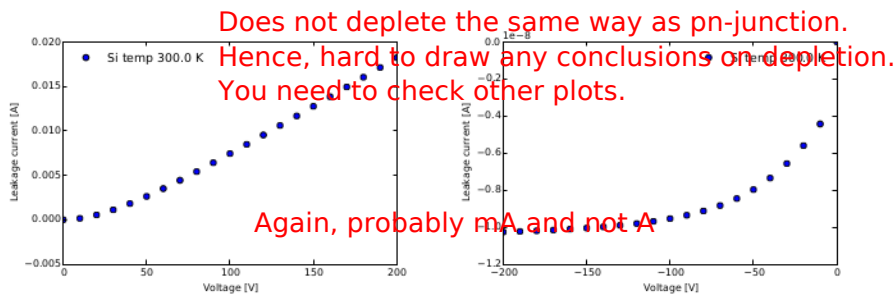


**Figure 3:** IV curve for the forward (left) and reverse (right) bias for the Schottky diode.

## References

- [1] Richard Brenner. *Basic Tracking Devices*. Lecture given at "Research training course in Detector Technology for particle physics". Stockholms Universitet, 2015.
- [2] *GSS homepage*. 2015.
- [3] G.F. Knoll. *Radiation Detection and Measurement*. 3rd ed. John Wiley & Sons, 2000.